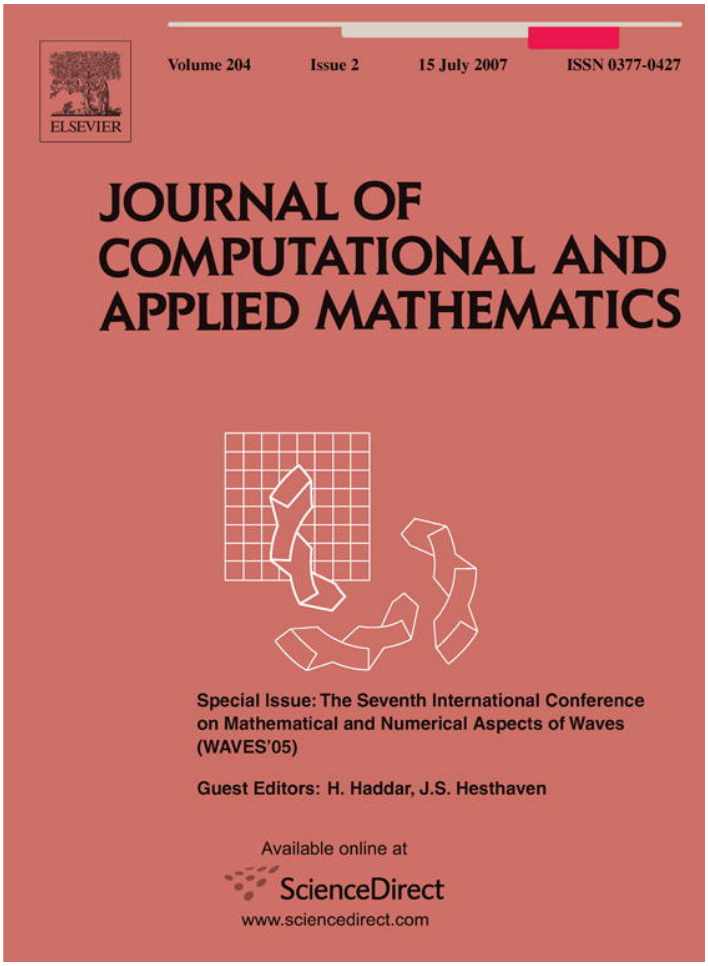

Available online at www.sciencedirect.com
ScienceDirect
Journal of Computational and Applied Mathematics 204 (2007) 256–267
JOURNAL OF COMPUTATIONAL AND APPLIED MATHEMATICS
www.elsevier.com/locate/cam

The inverse electromagnetic scattering problem for a partially coated dielectric

Fioralba Cakoni, David Colton, Peter Monk*

Department of Mathematical Sciences, University of Delaware, Newark, DE 19716, USA

Received 2 September 2005; received in revised form 2 February 2006

Abstract

We use the linear sampling method to determine the shape and surface conductivity of a partially coated dielectric infinite cylinder from knowledge of the far field pattern of the scattered TM polarized electromagnetic wave at fixed frequency. A mathematical justification of the method is provided based on the use of a complete family of solutions. Numerical examples are given showing the efficiency of our method.

Keywords: Inverse scattering problem; Electromagnetic waves; Mixed boundary value problems

1. Introduction

The use of dielectrics to coat a perfect conductor in an effort to help hostile objects avoid detection has a long history [9]. More recently, metallic coatings have been used in an effort to make benign dielectric objects look hostile, e.g., coating wooden decoys to make them appear as tanks to radar. In general, the obstacle is only partially coated and the extent and the composition of the coating is unknown. Such situations lead to mixed boundary value problems in scattering theory and particular difficulties arise in trying to solve the inverse problem since the boundary conditions on the scattering object are unknown. Inverse scattering problems of this type have been the subject of investigation by us in a series of papers [1–4]. In particular, our focus in these papers has been on the inverse problem of determining the shape and, if possible, the surface impedance or surface conductivity from a knowledge of the far field pattern of the scattered electromagnetic wave at fixed frequency.

The inverse scattering problem of determining the shape and surface conductivity of a partially coated dielectric from far field data is considerably more difficult to solve than the complementary case of a partially coated perfect conductor. This is due to the fact that in case of a coated dielectric the waves can penetrate into the obstacle, thus leading to electromagnetic fields inside the scattering object. Indeed, in our first effort to solve this problem we were only able to provide a mathematical justification of our reconstruction algorithm for the case of the scattering of TE-polarized plane waves by an infinite cylinder [4]. In the present paper we continue our investigation of this problem. In particular, a mathematical basis is given for an algorithm that determines the shape of a partially coated dielectric in the case of TM-polarized plane waves. This is accomplished by avoiding the need to solve an interior

* Corresponding author. Tel.: +1 302 831 1873; fax: +1 302 831 4511.
E-mail addresses: cakoni@math.udel.edu (F. Cakoni), colton@math.udel.edu (D. Colton), monk@math.udel.edu (P. Monk).

0377-0427/$ - see front matter © 2006 Elsevier B.V. All rights reserved.
doi:10.1016/j.cam.2006.03.026

transmission problem for an elliptic equation and instead relying on the construction of a special complete family of solutions. We follow this approach since, at this time, the well-posedness of the interior transmission problem remains an open problem. Unfortunately, this approach does not allow us to justify the method for determining the surface conductivity.

The plan of our paper is as follows. In Section 2 we formulate the direct and inverse scattering problem for a dielectric that is partially coated by a highly conductive layer in the TM case. We use the linear sampling method [5] to determine the shape and the scattering object, and give a heuristic formula for the surface conductivity. In Section 3 we test this formula, and the overall algorithm by some numerical examples. In particular, we shall provide an example showing that in the case of very large surface conductivity (e.g., a thick coating) it is possible to determine the portion of the boundary that is coated.

2. The TM polarized problem

We assume that the scatterer is an infinitely long cylinder with axis in the z-direction and assume that the incident electromagnetic field is a plane wave propagating in the direction perpendicular to the cylinder. Let the bounded domain $D \subset \mathbb{R}^2$ with Lipschitz boundary Γ be the cross section of the cylinder and assume that the exterior domain $D_e := \mathbb{R}^2 \setminus \overline{D}$ is connected. We denote by ν the outward unit normal to Γ defined almost everywhere on Γ. The boundary Γ has a Lipschitz dissection [10] $\Gamma = \Gamma_1 \cup \Pi \cup \Gamma_2$. Here Γ_1 corresponds to the uncoated part, Γ_2 corresponds to the coated part and Π is their common boundary. We assume that the dielectric is orthotropic.

If we consider incident waves such that the electric field is polarized parallel to the z-axis, then the electric fields have only a component in the z direction, i.e., the incident field E^i. Internal field E^{int} and scattered field E^s are given by $E^i = (0, 0, u^i)$, $E_0^{int} = (0, 0, v)$ and $E^s = (0, 0, u^s)$. Then the direct scattering problem for the electric field reads: given $f \in H^{1/2}(\Gamma)$, $h_1 \in H^{-1/2}(\Gamma_1)$ and $h_2 \in H^{-1/2}(\Gamma_2)$ find $v \in H^1(D)$ and $u^s \in H^1_{loc}(D_e)$ such that

$$\Delta u^s + k^2 u^s = 0 \quad \text{in } D_e, \tag{1}$$

$$\Delta v + k^2 n(x) v = 0 \quad \text{in } D, \tag{2}$$

$$v - u^s = f \quad \text{on } \Gamma, \tag{3}$$

$$\frac{\partial v}{\partial \nu} - \frac{\partial u^s}{\partial \nu} = h_1 \quad \text{on } \Gamma_1, \tag{4}$$

$$\frac{\partial v}{\partial \nu} - \frac{\partial u^s}{\partial \nu} = \mathrm{i}k\eta u^s + h_2 \quad \text{on } \Gamma_2, \tag{5}$$

$$\lim_{r\to\infty} \sqrt{r}\left(\frac{\partial u^s}{\partial r} - \mathrm{i}k u^s\right) = 0, \tag{6}$$

where $r = |x|$, $n \in C^1(\overline{D})$, $\Re(n) > 0$, $\Im(n) \geqslant 0$ and $\eta > 0$ is a constant called the *surface conductivity*. Here $H^1(D)$, $H^1_{loc}(D_e)$ are the usual Sobolev spaces, $H^{1/2}(\Gamma)$ and $H^{-1/2}(\Gamma)$ are the corresponding trace space and its dual, respectively, and $H^{1/2}(\Gamma_0) := \{u|_{\Gamma_0} : u \in H^{1/2}(\Gamma)\}$ for $\Gamma_0 \subset \Gamma$. For the scattering problem $f = u^i$ on Γ, $h_1 = \partial u^i/\partial \nu$ on Γ_1 and $h_2 = \partial u^i/\partial \nu + \mathrm{i}k\eta u^i$ on Γ_2. Note that due to the fact that the electric field is polarized parallel to the z-axis, only the $n = n_{3,3}$ entry of the matrix index of refraction $(n_{i,j})_{i,j=1}^3$ appears in Eq. (2).

Due to the compact embedding of $H^{1/2}(\Gamma_2)$ into $L^2(\Gamma_2)$, problem (1)–(6) can be seen as a compact perturbation of the same problem for $\eta = 0$ which is a particular case of the problem considered in [8]. Therefore the Fredholm alternative can be applied to (1)–(6). In particular, to prove the existence of a solution to (1)–(6) it suffices to show only the uniqueness.

Lemma 2.1. *Problem* (1)–(6) *has at most one solution.*

Proof. Applying Green's formula in D and $D_e \cap B_R$, where B_R is a ball of radius R about the origin, to v, $\overline{v}$ and u^s, $\overline{u}^s$, respectively, where u^s, v is a solution corresponding to $f = h_1 = h_2 = 0$ we obtain

$$\int_D (|\nabla v|^2 - k^2 n(x)|v|^2)\,\mathrm{d}y = \int_\Gamma \overline{v}\frac{\partial v}{\partial v}\,\mathrm{d}s$$
$$= \mathrm{i}k\eta \int_{\Gamma_2} |u^s|^2\,\mathrm{d}s + \int_{B_R} \overline{u^s}\frac{\partial u^s}{\partial v}\,\mathrm{d}s - \int_{D_e\cap B_R} (|\nabla u^s|^2 - k^2|u^s|^2)\,\mathrm{d}y$$

Hence $\Im(\int_{B_R} \overline{u}^s(\partial u^s/\partial v)\,\mathrm{d}s) \leqslant 0$ and the uniqueness follows from Rellich's lemma and the unique continuation principle [6]. □

Summarizing the above we have the following result:

Theorem 2.2. *Problem* (1)–(6) *has a unique solution* $v \in H^1(D)$, $u^s \in H^1_{\mathrm{loc}}(D_e)$ *which satisfies*

$$\|v\|_{H^1(D)} + \|u^s\|_{H^1(B_R\setminus\overline{D})} \leqslant C(\|f\|_{H^{1/2}(\Gamma)} + \|h_1\|_{H^{-1/2}(\Gamma_1)} + \|h_2\|_{H^{-1/2}(\Gamma_2)}) \tag{7}$$

for some positive constant C *depending on* R *but not on* f, h_1 *and* h_2.

We now consider the scattering problem (1)–(6) corresponding to incident plane waves, i.e., with $f := \mathrm{e}^{\mathrm{i}kx\cdot d}|_\Gamma$, $h_1 := (\partial \mathrm{e}^{\mathrm{i}kx\cdot d}/\partial v)|_{\Gamma_1}$ and $h_2 := (\partial \mathrm{e}^{\mathrm{i}kx\cdot d}/\partial v + \mathrm{i}k\eta \mathrm{e}^{\mathrm{i}kx\cdot d})|_{\Gamma_2}$, where $d \in \Omega := \{x \in \mathbb{R}^2 : |x| = 1\}$ denotes the incident direction.

The corresponding scattered field u^s has the asymptotic behavior [6]

$$u^s(x) = \frac{\mathrm{e}^{\mathrm{i}kr}}{\sqrt{r}} u_\infty(\hat{x}, d) + \mathrm{O}(r^{-3/2}),$$

as $r \to \infty$ where $u_\infty(\hat{x}, d)$ is defined on the unit circle Ω and is called the *far field pattern* of the radiating solution u^s. The inverse problem we consider here is to determine the shape of the scattering object D from a knowledge of the far field pattern $u_\infty(\hat{x}, d)$ for all incident plane waves $u^i := \mathrm{e}^{\mathrm{i}kx\cdot d}$, $d \in \Omega$, and all observation directions $\hat{x} \in \Omega$ (note that it suffices to know the far field pattern corresponding to all $d \in \Omega_1 \subset \Omega$ and all $\hat{x} \in \Omega_2 \subset \Omega$ [5]; of particular interest is the case $d = -\hat{x} \in \Omega_0 \subset \Omega$). We will also present a heuristic method for obtaining a lower bound for the surface conductivity η.

Our method for determining D is based on the construction of a special complete set of functions in $H^{1/2}(\Gamma) \times H^{-1/2}(\Gamma)$. In this construction certain values of the wave number k will play a special role. In particular, values of k for which

$$\left.\begin{aligned} &\Delta w + k^2 w = 0 \\ &\Delta v + k^2 n(x) v = 0 \end{aligned}\right\} \quad \text{in } D, \tag{8}$$

$$v - w = 0 \quad \text{on } \Gamma, \tag{9}$$

$$\frac{\partial v}{\partial v} - \frac{\partial w}{\partial v} = 0 \quad \text{on } \Gamma_1, \tag{10}$$

$$\frac{\partial v}{\partial v} - \frac{\partial w}{\partial v} = \mathrm{i}k\eta w \quad \text{on } \Gamma_2 \tag{11}$$

has a nontrivial solution $u \in H^1(D)$ and $v \in H^1(D)$ such that $\Delta v \in L^2(D)$ are called *transmission eigenvalues*. The following lemma shows that transmission eigenvalues can only exist when $\Im(n) = 0$.

Lemma 2.3. *If* $\Im(n(x_0)) > 0$ *at* $x_0 \in D$ *then transmission eigenvalues do not exist.*

Proof. Let v, w be a solution to (8)–(11). Applying Green's theorem to v, $\overline{v}$, making use of the boundary conditions and again applying Green's theorem to w, $\overline{w}$ we obtain

$$ik^2 \int_D \Im(n)|v|^2 \, dy = \int_\Gamma \left(v \frac{\partial \overline{v}}{\partial \nu} - \overline{v} \frac{\partial v}{\partial \nu} \right) ds = -2ik\eta \int_{\Gamma_2} |w|^2 \, ds.$$

Hence $\int_D \Im(n)|v|^2 \, dy = 0$ and $\int_{\Gamma_2} |w|^2 \, ds = 0$. Since $\Im(n) > 0$ in a small ball $B_{x_0} \subset D$, from the first equality we obtain that $v = 0$ in B_{x_0}, whence by unique continuation $v \equiv 0$ in D. From the boundary conditions and the integral representation formula w also vanishes in D. □

Note that in the case when $\Im(n) = 0$ and $\Gamma_2 = \Gamma$ (fully coated obstacle) from the above proof we have that $w = 0$ on Γ and hence the transmission eigenvalues form a subset of the *Dirichlet eigenvalues* for the Helmholtz equation $\Delta u + k^2 n(x) u = 0$ in D subject to the boundary condition $u = 0$ on Γ. We now recall that a Herglotz wave function with kernel $g \in L^2(\Omega)$ is an entire solution of the Helmholtz equation defined by

$$v_g(x) = \int_\Omega e^{-ikx \cdot d} g(d) \, ds(d), \quad x \in \mathbb{R}^2. \tag{12}$$

The following theorem plays an important role in the analysis of the inverse problem. We consider the space

$$V(D) := \{ v \in H^1(D) : \Delta v + k^2 n(x) v = 0 \quad \text{in } D \}$$

and define the subset of $H^{1/2}(\Gamma) \times H^{-1/2}(\Gamma)$ by

$$\mathcal{W} := \left\{ \left(v_g - v, \frac{\partial}{\partial \nu}(v_g - v) + ik\tilde{\eta} v_g \right) : g \in L^2(\Omega), v \in V(D) \right\},$$

where $\tilde{\eta} = \eta$ on Γ_2, $\tilde{\eta} = 0$ on Γ_1, and v_g is a Herglotz wave function with kernel g.

Theorem 2.4. *Suppose that k is neither a Dirichlet eigenvalue nor a transmission eigenvalue. Then $\mathcal{W}$ is dense in $H^{1/2}(\Gamma) \times H^{-1/2}(\Gamma)$.*

Proof. Let $\varphi \in H^{-1/2}(\Gamma)$ and $\psi \in H^{1/2}(\Gamma)$ be such that

$$\int_\Gamma (v_g - v) \varphi \, ds + \int_\Gamma \left[\frac{\partial}{\partial \nu}(v_g - v) + ik\tilde{\eta} v_g \right] \psi \, ds = 0 \tag{13}$$

for all $g \in L^2(\Omega)$ and $v \in V(D)$. Setting first $v = 0$ and interchanging the order of integrations we obtain

$$\int_\Omega g(\hat{x}) \int_\Gamma \left\{ \varphi(y) e^{-iky \cdot \hat{x}} + \psi(y) \left[\frac{\partial e^{-iky \cdot \hat{x}}}{\partial \nu} + ik\tilde{\eta} e^{-iky \cdot \hat{x}} \right] \right\} ds(y) \, ds(\hat{x}) = 0$$

for all $g \in L^2(\Omega)$ and hence

$$\int_\Gamma \varphi(y) e^{-iky \cdot \hat{x}} \, ds(y) + \int_\Gamma \psi(y) \left[\frac{\partial e^{-iky \cdot \hat{x}}}{\partial \nu} + ik\tilde{\eta} e^{-iky \cdot \hat{x}} \right] ds(y) = 0.$$

The left hand side of the above expression is the far field pattern of the potential

$$u(x) = \int_\Gamma \varphi(y) \Phi(x, y) \, ds(y) + \int_\Gamma \psi(y) \frac{\partial \Phi(x, y)}{\partial \nu} \, ds(y) + ik \int_\Gamma \tilde{\eta} \psi(y) \Phi(x, y) \, ds(y),$$

where $\Phi(x, z) := (i/4) H_0^{(1)}(k|x - z|)$ with $H_0^{(1)}$ being a Hankel function of the first kind of order zero. Note that u is in $H^1(D)$ and $H^1_{\text{loc}}(D_e)$, and u satisfies the Helmholtz equation in D and D_e. Therefore we conclude that $u(x) = 0$

in D_e. Using the jump relations for single and double layer potentials [10] we then obtain

$$\psi = -u^-, \quad \varphi = \frac{\partial u^-}{\partial \nu} + ik\tilde{\eta}u^- \text{ on } \Gamma, \tag{14}$$

where the superscript $-$ indicates that the limit is obtained by approaching the boundary Γ from D.

Next we set $g = 0$ in (13), use (14) and Green's formula to obtain

$$\begin{aligned} 0 &= \int_\Gamma \left[u^- \frac{\partial v}{\partial \nu} - v \left(\frac{\partial u^-}{\partial \nu} + ik\tilde{\eta}u^- \right) \right] ds \\ &= k^2 \int_D (1-n)uv\, dx - ik \int_\Gamma \tilde{\eta} uv\, ds. \end{aligned} \tag{15}$$

Now let $w \in H^1(D)$ be the unique solution of $\Delta w + k^2 n w = k^2(1-n)u$ in D together with $w = 0$ on Γ. Applying Green's theorem and (15) yields

$$\int_\Gamma v \frac{\partial w}{\partial \nu}\, ds = k^2 \int_D (1-n)uv\, dx = ik \int_\Gamma \tilde{\eta} uv\, ds.$$

Hence $\int_\Gamma v(\partial w/\partial \nu - ik\tilde{\eta}u)\, ds = 0$ for all $v \in V(D)$ which implies that $\partial w/\partial \nu - ik\tilde{\eta}u = 0$ on Γ. Note that for any $f \in H^{1/2}(\Gamma)$ one can find a unique $v \in V(D)$ such that $v|_\Gamma = f$ since k is not a Dirichlet eigenvalue. We observe that u and $\tilde{w} = u + w$ satisfy

$$\left.\begin{aligned} &\Delta u + k^2 u = 0 \\ &\Delta \tilde{w} + k^2 n(x) \tilde{w} = 0 \end{aligned}\right\} \quad \text{in } D, \tag{16}$$

$$\tilde{w} - u = 0 \quad \text{on } \Gamma, \tag{17}$$

$$\frac{\partial \tilde{w}}{\partial \nu} - \frac{\partial u}{\partial \nu} = 0 \quad \text{on } \Gamma_1, \tag{18}$$

$$\frac{\partial \tilde{w}}{\partial \nu} - \frac{\partial u}{\partial \nu} = ik\eta u \quad \text{on } \Gamma_2, \tag{19}$$

whence $u = \tilde{w} = 0$ provided that k is not a transmission eigenvalue. Therefore (14) implies $\varphi = \psi = 0$ which proves the result. □

The following lemma is a technical tool we need for solving the inverse problem. We define the closed subset $H(\Gamma)$ of $H^{1/2}(\Gamma) \times H^{-1/2}(\Gamma)$ by

$$H(\Gamma) = \left\{ \left(u|_\Gamma, \left. \frac{\partial u}{\partial \nu} + ik\tilde{\eta}u \right|_\Gamma \right) : u \in H^1(D), \quad \Delta u + k^2 u = 0 \right\}.$$

Then we consider the bounded operator $\mathcal{B} : H(\Gamma) \to L^2(\Omega)$ which maps an element of $H(\Gamma)$ onto the far field pattern u_∞ of the solution (v, u^s) to (1)–(6) with boundary data $f := u|_\Gamma$, $h_1 := \partial u/\partial \nu + ik\tilde{\eta}u|_{\Gamma_1}$ and $h_2 := \partial u/\partial \nu + ik\tilde{\eta}u|_{\Gamma_2}$.

Lemma 2.5. *The operator $\mathcal{B} : H(\Gamma) \to L^2(\Omega)$ is compact, injective and has dense range providing that k is neither a Dirichlet eigenvalue nor a transmission eigenvalue.*

Proof. Compactness is a simple consequence of the fact that $\mathcal{B}$ can be seen as a composition of the continuous solution operator to (1)–(6) with the compact operator which maps a radiating solution to its far field (c.f. [6]).

Next we show the injectivity of $\mathcal{B}$. Let $\mathcal{B}(\varphi, \psi) = 0$ where $\varphi = u|_\Gamma$ and $\psi = \partial u/\partial \nu + ik\tilde{\eta}u|_\Gamma$ for $u \in H^1(D)$ such that $\Delta u + k^2 u = 0$, and let (v, u^s) be the solution to (1)–(6) corresponding to this boundary data. Hence $u^s \equiv 0$ for $x \in \mathbb{R}^2 \setminus \overline{D}$. This implies that v satisfies $\Delta v + k^2 n v = 0$ in D, $v = \varphi$ and $\partial v/\partial \nu = \psi$ on Γ. Hence (v, u) solves (16)–(19) and since k is not a transmission eigenvalue we have that $v \equiv 0$ and consequently $\varphi = \psi \equiv 0$.

Finally it remains to show that $\mathscr{B}(H^1(D))$ is dense in $L^2(\Omega)$. It is easily verifiable that the far field patterns of radiating cylindrical wave functions $H_m^{(1)}(kr)\mathrm{e}^{\pm \mathrm{i}m\phi}$, $m = 0, 1, \ldots$, where $H_m^{(1)}$ are the Hankel functions of the first kind of order m, form a complete set in $L^2(\Omega)$. For a arbitrarily small ε and fixed m from Theorem 2.4 we can find a Herglotz function v_{g_ε} and a $v_\varepsilon \in V(D)$ such that

$$\begin{cases} v_\varepsilon - H_m^{(1)}(kr)\mathrm{e}^{\pm \mathrm{i}m\phi} = v_{g_\varepsilon} + \alpha_\varepsilon, \\ \dfrac{\partial v_\varepsilon}{\partial \nu} - \left(\dfrac{\partial}{\partial \nu} + \mathrm{i}k\tilde{\eta}\right) H_m^{(1)}(kr)\mathrm{e}^{\pm \mathrm{i}m\phi} = \dfrac{\partial v_{g_\varepsilon}}{\partial \nu} + \mathrm{i}k\tilde{\eta} v_{g_\varepsilon} + \beta_\varepsilon \end{cases} \tag{20}$$

on Γ where $\|\alpha_\varepsilon\|_{H^{1/2}(\Gamma)} \leqslant \varepsilon$ and $\|\beta_\varepsilon\|_{H^{-1/2}(\Gamma)} \leqslant \varepsilon$. We observe that v_ε and $H_m^{(1)}(kr)\mathrm{e}^{\pm \mathrm{i}m\phi}$ solve the transmission problem (1)–(6) with data given by the right hand side of (20). Hence the far field pattern u_∞^ε of the scattered field u_ε^s corresponding to v_{g_ε} as incident wave approximate the far field pattern of $H_m^{(1)}(kr)\mathrm{e}^{\pm \mathrm{i}m\phi}$ with discrepancy $C\varepsilon$ for some positive constant C because the far field pattern depends continuously on the scattered wave which on the other hand depends continuously on the data. Noticing that u_∞^ε is in the range of $\mathscr{B}$ proves the lemma. □

The method we will use here to determine D and η is based on solving the *far field equation*

$$(Fg)(\hat{x}) = \gamma \mathrm{e}^{-\mathrm{i}k\hat{x}\cdot z}, \quad g \in L^2(\Omega), \quad z \in D \tag{21}$$

where $\gamma = \mathrm{e}^{\mathrm{i}\pi/4}/\sqrt{8\pi k}$ and $F : L^2(\Omega) \to L^2(\Omega)$ is the *far field operator* given by $Fg(\hat{x}) := \int_\Omega u_\infty(\hat{x}, d)g(d)\,\mathrm{d}s(d)$. Note that $\gamma \mathrm{e}^{-\mathrm{i}k\hat{x}\cdot z}$ is the far field pattern of the fundamental solution $\Phi(x, z)$.

Theorem 2.6. *Assume that k is neither a transmission eigenvalue nor a Dirichlet eigenvalue. Then we have*:

(1) *For $z \in D$ and every $\varepsilon > 0$ there exists a solution $g_\varepsilon^z \in L^2(\Omega)$ of the inequality $\|Fg_\varepsilon^z - \gamma \mathrm{e}^{-\mathrm{i}k\hat{x}\cdot z}\|_{L^2(\Omega)} < \varepsilon$ such that $\lim_{z\to\Gamma}\|g_\varepsilon^z\|_{L^2(\Omega)} = \infty$ and $\lim_{z\to\Gamma}\|v_{g_\varepsilon^z}\|_{H^1(D)} = \infty$, where $v_{g_\varepsilon^z}$ is the Herglotz wave function with kernel g_ε^z.*
(2) *For $z \in \mathbb{R}^2\backslash\overline{D}$ and every $\varepsilon > 0$ and $\delta > 0$ there exists a solution $g_{\varepsilon,\delta}^z = \in L^2(\Omega)$ of the inequality $\|Fg_{\varepsilon,\delta}^z - \gamma \mathrm{e}^{-\mathrm{i}k\hat{x}\cdot z}\|_{L^2(\Omega)} < \varepsilon + \delta$ such that $\lim_{\delta\to 0}\|g_{\varepsilon,\delta}^z\|_{L^2(\Omega)} = \infty$ and $\lim_{\delta\to 0}\|v_{g_{\varepsilon,\delta}^z}\|_{H^1(D)} = \infty$, where $v_{g_{\varepsilon,\delta}^z}$ is the Herglotz wave function with kernel $g_{\varepsilon,\delta}^z$.*

Proof. Let $z \in D$. Given $\varepsilon > 0$, from Theorem 2.4 there exists $v_{g_\varepsilon^z}$ with $g_\varepsilon := g_\varepsilon^z \in L^2(\Omega)$ and $v_\varepsilon \in V(D)$ such that

$$\left.\begin{aligned} & v_\varepsilon - \Phi(\cdot, z) = v_{g_\varepsilon} + \alpha_\varepsilon \\ & \frac{\partial v_\varepsilon}{\partial \nu} - \frac{\partial \Phi(\cdot, z)}{\partial \nu} - \mathrm{i}k\tilde{\eta}\Phi(\cdot, z) = \frac{\partial v_{g_\varepsilon}}{\partial \nu} + \mathrm{i}k\tilde{\eta} v_{g_\varepsilon} + \beta_\varepsilon \end{aligned}\right\} \quad \text{on } \Gamma, \tag{22}$$

where $\|\alpha_\varepsilon\|_{H^{1/2}(\Gamma)} \leqslant \varepsilon$ and $\|\beta_\varepsilon\|_{H^{-1/2}(\Gamma)} \leqslant \varepsilon$. We note that Fg_ε is the far field pattern of the solution to (1)–(6) with $f := v_{g_\varepsilon}|_\Gamma$, $h := (\partial v_{g_\varepsilon}/\partial \nu)|_\Gamma$ and $g := (\partial v_{g_\varepsilon}/\partial \nu + \mathrm{i}k\eta v_{g_\varepsilon})|_\Gamma$, and $\gamma \mathrm{e}^{-\mathrm{i}k\hat{x}\cdot z}$ is the far field pattern of $\Phi(\cdot, z)$ which together with v_ε solves (1)–(6) with boundary data of the right hand side of (22). Hence from estimate (7) and the fact that the far field pattern depends continuously on the scattered field we obtain $\|Fg_\varepsilon - \gamma \mathrm{e}^{-\mathrm{i}k\hat{x}\cdot z}\|_{L^2(\Omega)} < C\varepsilon$ for some positive constant C. Now let z approach the boundary Γ from inside. Using (7) for the solution v_ε and $\Phi(\cdot, z)$ of the transmission problem with the transmission condition (22), we obtain

$$\begin{aligned} \|v_\varepsilon\|_{H^1(D)} + \|\Phi(\cdot, z)\|_{H^1(B_R\backslash\overline{D})} &\leqslant C_0\left(\|v_{g_\varepsilon}\|_{H^{1/2}(\Gamma)} + \left\|\frac{\partial v_{g_\varepsilon}}{\partial \nu}\right\|_{H^{-1/2}(\Gamma)} + \varepsilon\right) \\ &\leqslant C_1(\|v_{g_\varepsilon}\|_{H^1(D)} + \varepsilon), \end{aligned}$$

where C_0, C_1 are two positive constants independent of z and ε. Since ε is fixed we finally have that $\|v_{g_\varepsilon(\cdot,z)}\|_{H^1(D)} \to \infty$ and $\|g_\varepsilon(\cdot, z)\|_{L^2(\Omega)} \to \infty$ as $z \to \Gamma$. Next let us consider $z \in \mathbb{R}^2\backslash\overline{D}$. For these points $\gamma \mathrm{e}^{-\mathrm{i}k\hat{x}\cdot z}$ does not belong to the range of the operator $\mathscr{B}$ defined in Lemma 2.5 because $\Phi(\cdot, z)$ is not an H^1-solution to the Helmholtz equation in

the exterior of D. But, from Lemma 2.5, using Tikhonov regularization, we can construct a regularized solution of the equation

$$\mathscr{B}(\varphi, \psi) = \gamma e^{-ik\hat{x}\cdot z}. \tag{23}$$

In particular, if

$$(\varphi_z^\alpha, \psi_z^\alpha) = \left(u_z^\alpha|_\Gamma, \ \frac{\partial u_z^\alpha}{\partial \nu} + ik\tilde{\eta} u_z^\alpha \Big|_\Gamma \right) \in H(\Gamma),$$

with $u_z^\alpha \in H^1(D)$ being a solution of the Helmholtz equation is a regularized solution of (23) corresponding to the regularization parameter α chosen by a regular regularization strategy (e.g., the Morozov discrepancy principle [6]), we have $\|\mathscr{B}((\varphi_z^\alpha, \psi_z^\alpha)) - \gamma e^{-ik\hat{x}\cdot z}\|_{L^2(\Omega)} < \delta$, for an arbitrary small but fixed $\delta > 0$, and

$$\lim_{\alpha\to 0} (\|\varphi_z^\alpha\|_{H^{1/2}(\partial D)} + \|\psi_z^\alpha\|_{H^{-1/2}(\partial D)}) = \lim_{\alpha\to 0} \|u_z^\alpha\|_{H^1(D)} = \infty. \tag{24}$$

Note that in this case we have that $\alpha \to 0$ as $\delta \to 0$. Then the second part of the theorem follows from the fact that u_z^α can be approximated arbitrarily closely in the $H^1(D)$ norm by a Herglotz wave function v_g [7], from the continuity of $\mathscr{B}$ and the fact that $Fg = \mathscr{B}(v_g|_\Gamma, \partial v_g/\partial \nu + ik\tilde{\eta} v_g|_\Gamma)$. This ends the proof. □

Theorem 2.6 provides a partial mathematical justification of the *linear sampling method* for determining D. In particular, the boundary of D is characterized as the set of points where $\|g\|_{L^2(\Omega)}$ becomes large for $g \in L^2(\Omega)$ being a (regularized) solution of the far field (21). However, it remains to show that the regularized solution of the far field equation in fact approximates the functions g_ε^z and $g_{\varepsilon,\delta}^z$ whose existence is established in Theorem 2.6.

Having reconstructed D, we next need a formula for η. Unfortunately the preceding theory does not allow a rigorous justification of the upcoming formula since we have avoided analyzing the interior transmission problem. Proceeding heuristically as in [4] we can derive a suitable formula. Suppose z is a fixed point in D, $\Im(n) = 0$ and assume that k is neither a Dirichlet eigenvalue nor a transmission eigenvalue. Then if $v_{g_\varepsilon^z}$ denotes a herglotz wave function with kernel $g_\varepsilon^z \in L^2(\Omega)$ that is a suitable approximate solution of the far field (21) we have

$$\eta \approx -\frac{2k\pi|\gamma|^2 + \Im(v_{g_\varepsilon^z}(z))}{k\|(v_{g_\varepsilon^z} + \Phi(\cdot, z))\|^2_{L^2(\Gamma_2)}}. \tag{25}$$

Note that since in practice Γ_2 is unknown, in general we must replace Γ_2 by Γ in (25). In this case (25) only yields a *lower bound* for the unknown parameter η.

3. Numerical examples

We shall now present some simple numerical examples in two dimensions to demonstrate the performance of our proposed scheme. The choice of scatterers and general approach is similar to that in [4] where details of the method may be found. Briefly, we choose a particular scatterer and surface conductivity. Then we predict the far field pattern using a cubic finite element method terminated by a perfectly matched layer. After the addition of noise (the method for doing this and noise level are the same as in [4]), the approximate far field data are used to reconstruct the boundary of the scatterer. This is accomplished by discretizing the far field equation (21) using as quadrature points the measurement directions (see below), and using Tikhonov regularization and Morozov's principle. The Morozov parameter (the same for all sampling points z) is the error in the far field due to the addition of noise. Then using sampling points z in the neighborhood of the unknown scatterer we can use the discrete approximation to $1/\|g\|_{L^2(\Omega)}$ as an indicator function for the boundary of the scatterer. This involves choosing a particular contour value C so that the reconstructed scatterer is given by the curve where $1/\|g\|_{L^2(\Omega)} = C$. We shall comment more on the choice of C shortly. Once the boundary of the scatterer has been approximated, we use (25) to approximate the surface conductivity η. As in [4] the relevant norm on Γ_2 is computed using the trapezoidal rule with 100 integration points and we use the single point $z = (0, 0)^T$.

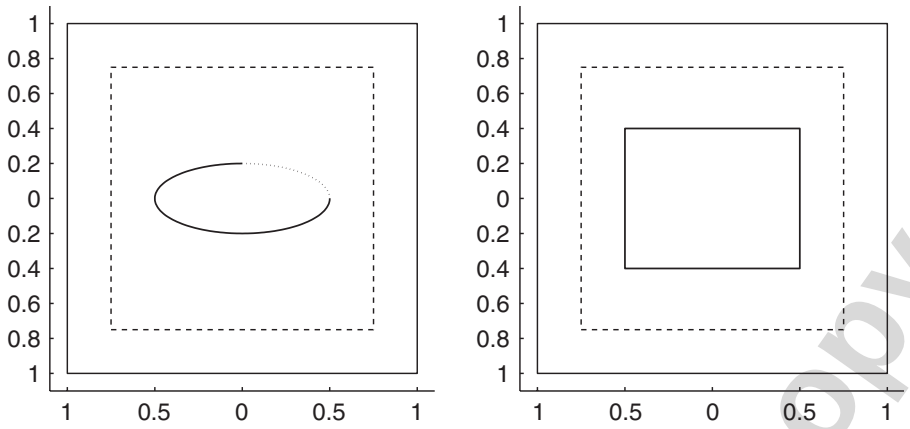

Fig. 1. The two simple scatterers used in this paper. For the ellipse we mark as a dark line the portion of the boundary used for the partially coated results. In both panels the dashed line shows the start of the perfectly matched layer that is used to terminate the computational domain. The entire region is meshed using the finite element method for the forward problem.

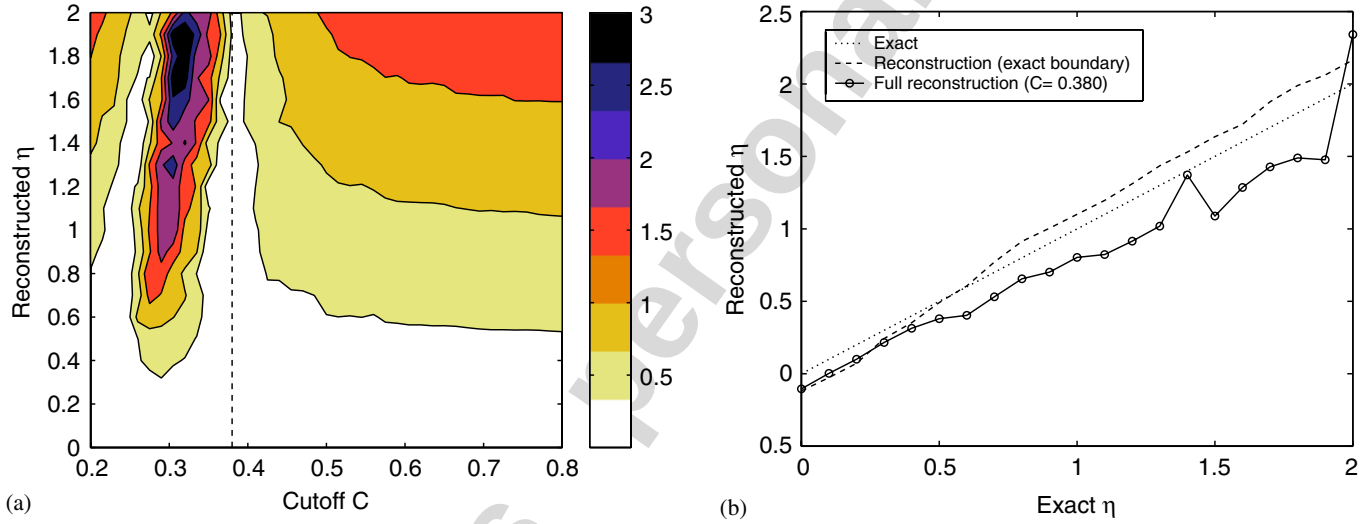

Fig. 2. Results for reconstructing the surface conductivity of a fully coated ellipse at $k = 5$. The boundary is shown in Fig. 1. In the left panel we show the error in the reconstructed conductivity η as a function of the exact η and the contour level C. The dotted line at $C = 0.38$ marks the optimal choice. Using this choice of contour level gives the results in the right hand panel where we also show the results of using (25) knowing the exact boundary. Most of the error in the reconstruction of η results from the reconstruction of the boundary of the ellipse: (a) error in the reconstruction; (b) reconstruction for $C = 0.38$.

The two simple scatterers considered here are an ellipse and a rectangle shown in Fig. 1. Using the far field pattern for these figures we can compute the reconstruction of η. In the upcoming sections we show results computed using 21 values of the exact conductivity η between 0 and 2 and for 41 contour levels C between 0.2 and 0.8. In all cases we use 61 incoming waves uniformly distributed in $[0, 2\pi]$ and 61 data points at the same angles.

3.1. Scattering by an ellipse

We start with a fully coated (i.e., η is constant on the entire boundary) ellipse and investigate the reconstruction of η for a range of η, for various choices of contour level C and for two wave numbers. We start with $k = 5$. In Fig. 2(a) we show a contour map of the error in the reconstruction measured in the maximum norm as a function of the exact η and contour level C. We would like to have a single choice of contour level independent of the exact value of η for the reconstruction and in the figure we mark a reasonable choice (the choice $C = 0.380$ minimizes the infinity norm of the

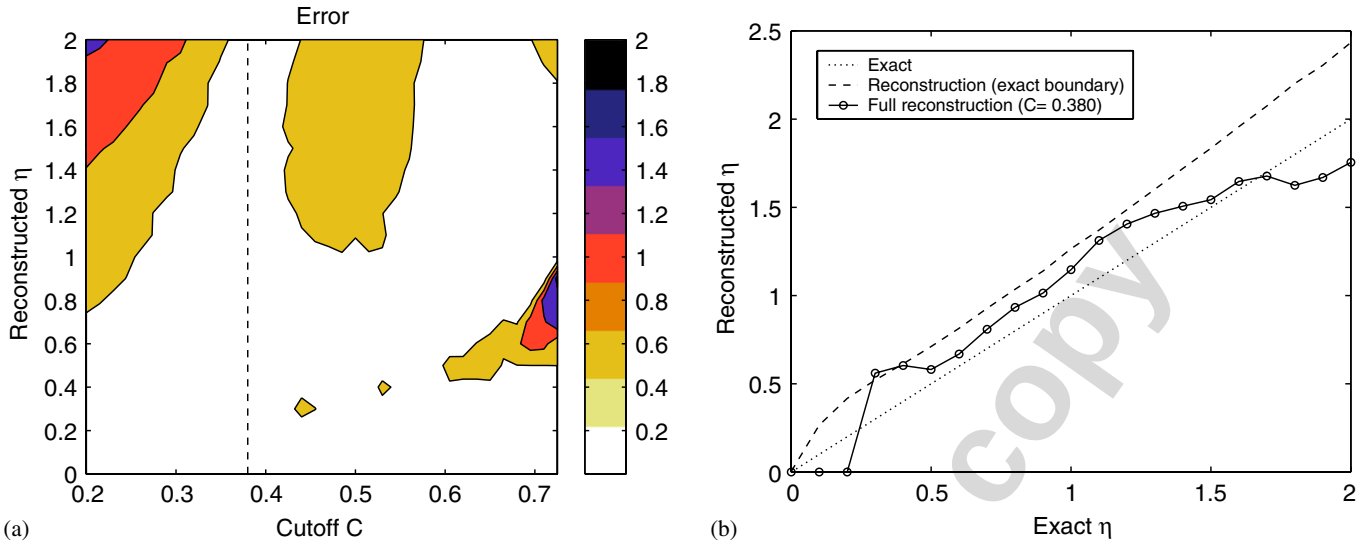

Fig. 3. Results for reconstructing the surface conductivity of a fully coated ellipse at $k = 10$. See the caption to Fig. 2 for an explanation: (a) error in the reconstruction; (b) reconstruction for $C = 0.38$.

reconstruction over the range indicated). This choice lies in a valley of the error surface for almost its whole length. In Fig. 2(b) we show the reconstruction of η for the chosen contour level as the exact value of η varies. We also show the reconstruction using (25) but with the exact boundary. Using the exact boundary gives a much better reconstruction so, in this case, the (absolute) error in the reconstruction of η for the boundary given by the linear sampling method is mostly due to the inexact reconstruction of the boundary. This example illustrates a problem with using a combination of the linear sampling method and (25) to reconstruct η: the method is sensitive to the choice of the contour level C. In [4] we found a heuristic criterion for choosing the contour level which worked well in the examples we have tried for the method of that paper, but no such heuristic is obvious for the method in this paper.

For $k = 10$ the behavior of the algorithm is broadly similar to the case when $k = 5$. In this case the far field data are less accurate since we used the same finite element grid for solving the forward problem for both wave numbers. Results are shown in Fig. 3. There is still a choice of the contour level C that provides a reasonable reconstruction throughout the range of η. The value of the optimal contour level is $C = 0.395$ which is roughly that used when $k = 5$ so that a single choice of contour level could be used for both wave numbers. Oddly the reconstruction using the exact boundary overestimates η throughout the range, perhaps due to the less accurate far field data.

3.2. Scattering by a rectangle

Next we investigate the fully coated rectangle where η is constant on the entire surface of the rectangle. We perform the reconstruction for the same choice of wave numbers and other parameters as in the previous subsection. In [4] we found that the rectangle presented a more difficult reconstruction problem than the ellipse, and that is also the case here. When $k = 5$ we show the results of reconstructing η in Fig. 4. In the left hand panel we see that there is no longer a choice of contour level C that provides a small reconstruction error for all η (i.e., lies in a valley of the error surface). We have marked $C = 0.485$ as a dashed line and this minimizes the maximum norm error in the reconstruction over the range of η here. In the right hand panel we show the reconstruction of η using the optimal contour level as well as a reconstruction using the exact boundary. Clearly, the overall error in the reconstruction is almost entirely due to the preliminary reconstruction of the boundary of the scatterer.

One way to improve the reconstruction by the linear sampling method is to increase the wave number. In Fig. 5 we show the results of reconstructing the surface conductivity of the rectangle when $k = 10$. Note that in this case we used a finite element mesh of half the mesh size compared to that used when $k = 5$. The reconstruction of η is now improved. Unfortunately the optimal contour level C is now markedly smaller than for the case of the ellipse or the rectangle at $k = 5$ indicating that the contour level needs to be chosen depending on the scatterer, the wave number and the viewing aperture.

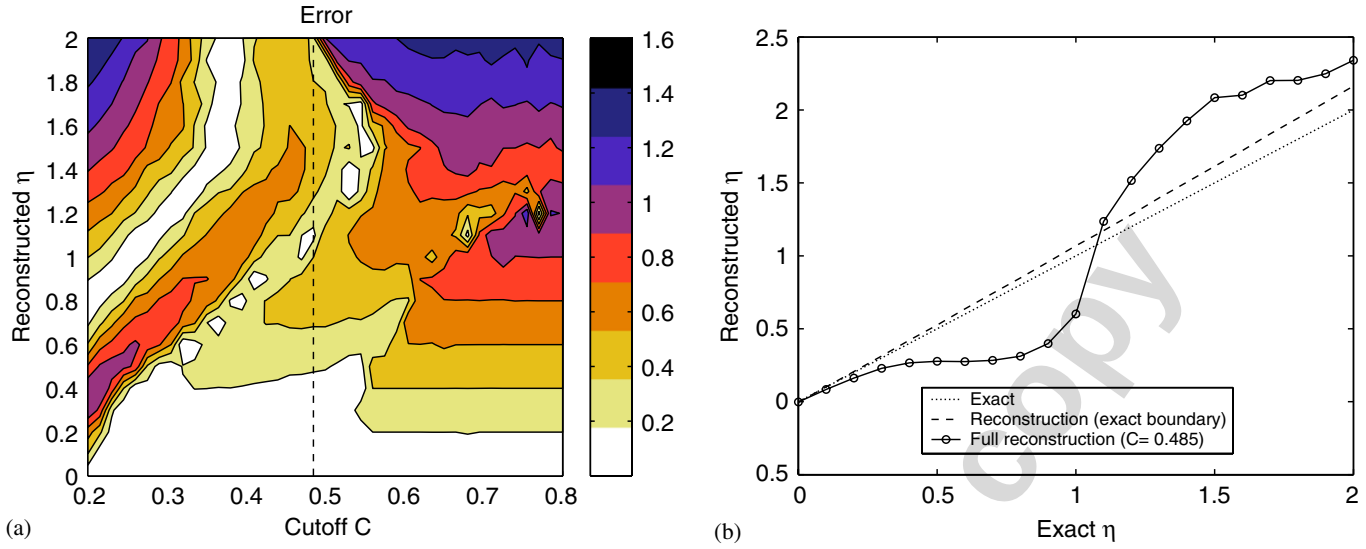

Fig. 4. Results for reconstructing the surface conductivity of a fully coated rectangle at $k = 5$. See the caption to Fig. 2 and the text for an explanation: (a) error in the reconstruction; (b) reconstruction for $C = 0.485$.

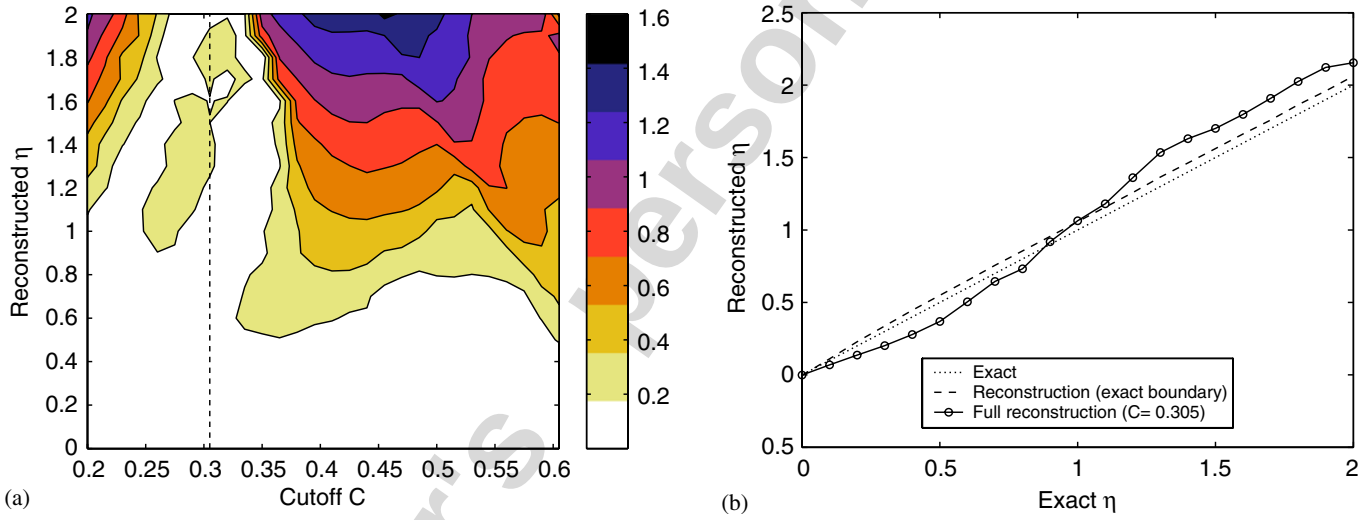

Fig. 5. Results for reconstructing the surface conductivity of a fully coated rectangle at $k = 10$. See the caption to Fig. 2 and the text for an explanation: (a) error in the reconstruction; (b) reconstruction for $C = 0.305$.

3.3. A partially coated scatterer

Here we show some results for applying (25) when Γ_2 is a proper subset of Γ. In particular, we use the partially coated subset of the boundary of the ellipse shown in Fig. 1. The results are shown in Fig. 6. As expected, the reconstruction underestimates the true value of η when $\Gamma \neq \partial D$.

If the surface conductivity η is large, Eq. (22) suggests that for any z inside the scatterer $v_{g_\varepsilon^z} + \Phi \approx 0$ on the coated portion of Γ (i.e., where η is large). Thus we should be able to use this quantity as an indicator for Γ_2. Numerical experiments (not shown here) show that the choice $z = (0, 0)^T$ used for computing η does not work well to determine this conducting boundary. Instead we compute $v_{g^z} + \Phi$ for z closer to the reconstructed boundary. For the ellipse we choose $z = (0.3\cos(\pi(j-1)/10), 0.1\sin(\pi(j-1)/10))^T$, $j = 1, \ldots, 10$, and plot a contour map of the average value of $|v_{g^z} + \Phi|$. In Fig. 7(a) we show the linear sampling method reconstruction of the partially coated ellipse when $k = 10$ and $\eta = 20$ on the coated portion of the boundary. In the right hand panel we show the average value of $|v_{g_\varepsilon^z} + \Phi|$ using

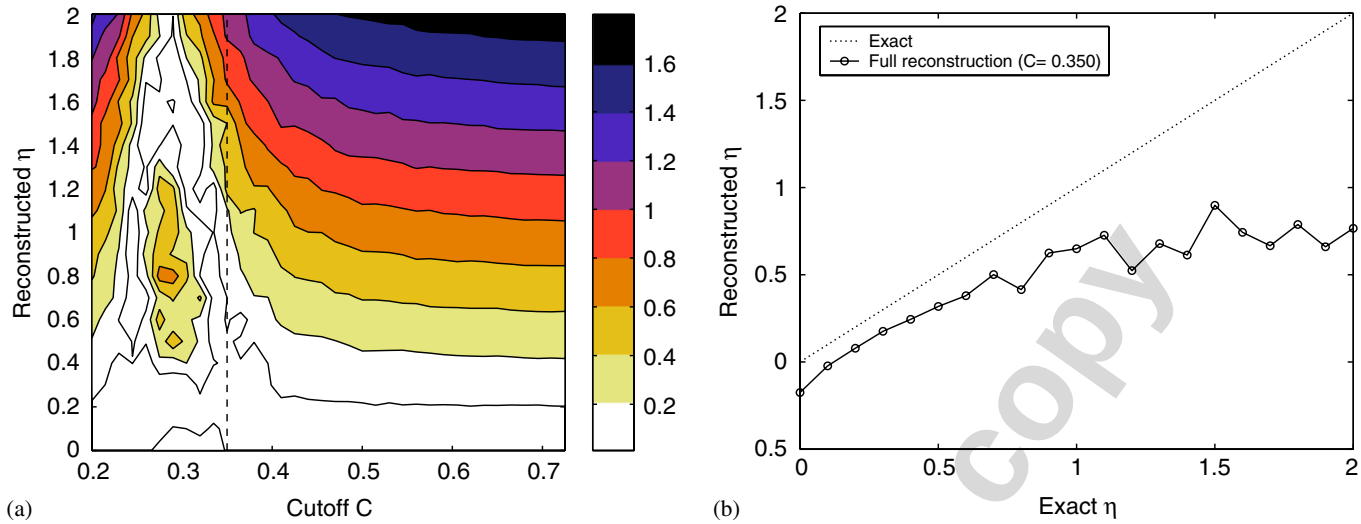

Fig. 6. Results for reconstructing the surface conductivity of a partially coated ellipse when $k = 5$. See the caption to Fig. 2 and the text for an explanation: (a) error in the reconstruction; (b) reconstruction for $C = 0.35$.

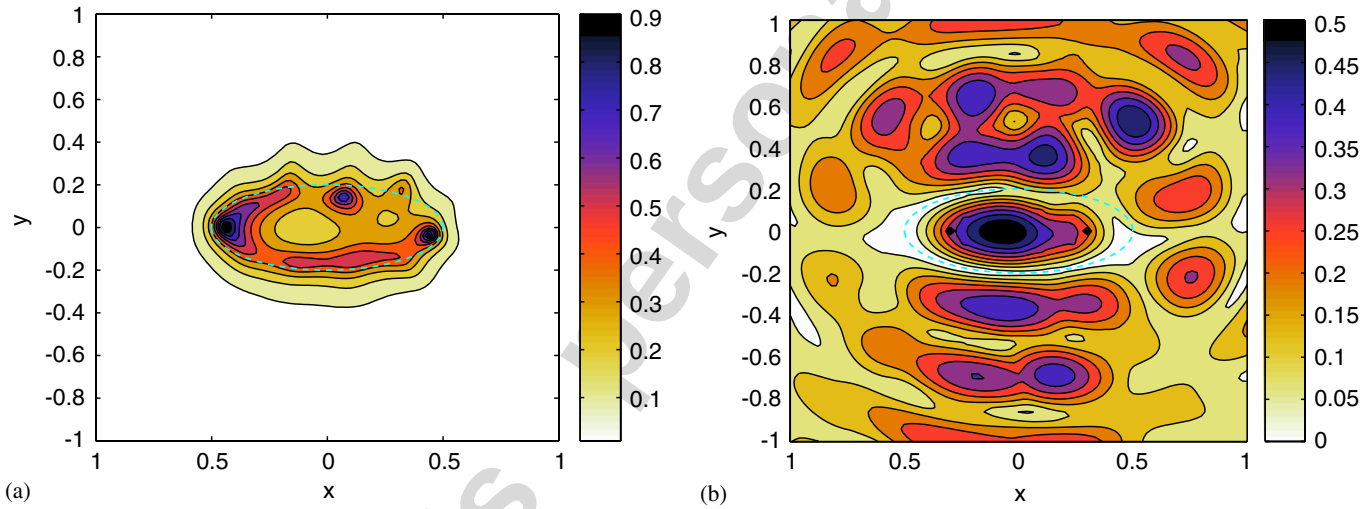

Fig. 7. Reconstruction of the boundary Γ_2 of the ellipse shown in Fig. 1 when $\eta = 20$ on Γ_2 and $k = 5$. The left panel shows the indicator function $1/\|g\|_{L^2(\Omega)}$ from the basic linear sampling method. The right panel shows the average value of $|v_{g_\varepsilon^z} + \Phi|$ using 10 choices of z within the ellipse (see text). The conducting portion of the boundary is correctly located as a minimum of $|v_{g_\varepsilon^z} + \Phi|$. In both cases the dashed line shows the exact boundary ∂D: (a) reconstruction of ∂D; (b) reconstruction for Γ_2.

the 10 choices of z mentioned previously. Clearly, the minimum of this function does pick out the conducting portion of the boundary. Fig. 7(a) clearly shows that some feature of the boundary changes in the upper right quadrant of the reconstruction. But the use of $v_{g_\varepsilon^z} + \Phi$ gives an indicator for the portion of the boundary where the conductivity is high, thus giving a more precise statement about the nature of the domain.

4. Conclusion

We have shown how the linear sampling method may be used to reconstruct both the shape and the surface conductivity of an infinite cylinder in the case of TM polarized incident waves. Numerical results show that provided the shape of the scatterer is reconstructed sufficiently accurately, the proposed method can provide a reliable reconstruction of the surface conductivity. The main difficulty with the method (in the case of TM polarization) is the lack of a rigorous justification of the formula giving a lower bound for η and the necessity of making an accurate choice of the contour level parameter in the shape reconstruction problem.

Acknowledgments

We gratefully acknowledge the support of our research by the Air Force Office of Scientific Research under grant number FA9550-05-1-0127 and an NSF SCREMS grant number DMS-0322583.

References

[1] F. Cakoni, D. Colton, A uniqueness theorem for an inverse electromagnetic scattering problem in inhomogeneous anisotropic media, Proc. Edinburgh Math. Soc. 46 (2003) 293–314.
[2] F. Cakoni, D. Colton, The determination of the surface impedance of a partially coated obstacle from far field data, SIAM J. Appl. Math. 64 (2004) 709–723.
[3] F. Cakoni, D. Colton, P. Monk, The electromagnetic inverse scattering problem for partially coated Lipschitz domains, Proc. Roy Soc. Edinburgh 134A (2004) 661–682.
[4] F. Cakoni, D. Colton, P. Monk, The determination of the surface conductivity of a partially coated dielectric, SIAM J. Appl. Math. 65 (2005) 767–789.
[5] D. Colton, H. Haddar, M. Piana, The linear sampling method in inverse electromagnetic scattering theory, Inverse Problems 19 (2003) S105–S137.
[6] D. Colton, R. Kress, Inverse Acoustic and Electromagnetic Scattering Theory, second ed., Springer, Berlin, 1998.
[7] D. Colton, B.D. Sleeman, An approximation property of importance in inverse scattering theory, Proc. Edinburgh Math. Soc. 44 (2001) 449–454.
[8] P. Hähner, On the uniqueness of the shape of a penetrable, anisotropic obstacle, J. Comput. Appl. Math. 116 (2000) 167–180.
[9] D.J. Hoppe, Y. Rahmat-Samii, Impedance Boundary Conditions in Electromagnetics, Taylor & Francis Publishers, Washington DC, 1995.
[10] W. McLean, Strongly Elliptic Systems and Boundary Integral Equations, Cambridge University Press, Cambridge, 2000.